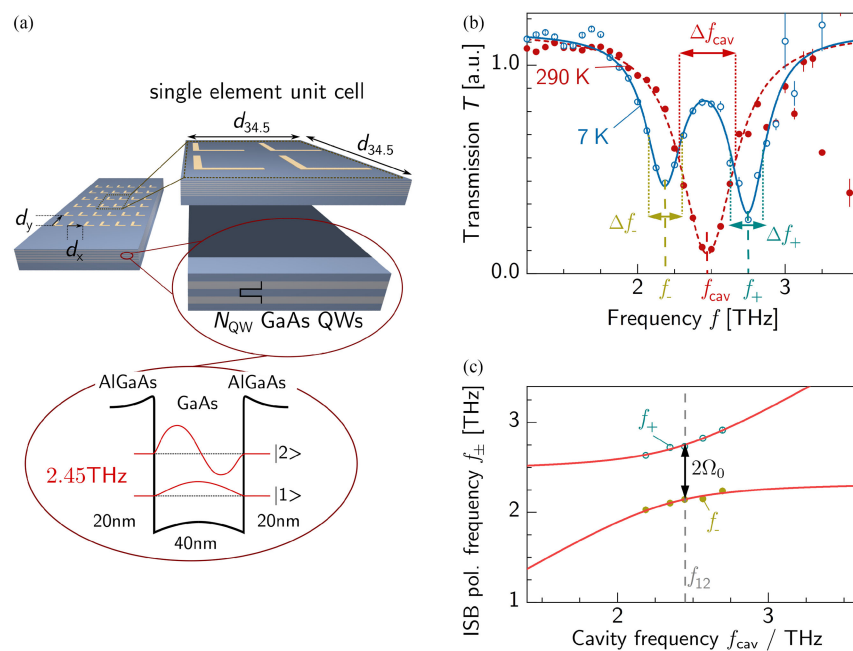


# Superradiant Ensembles of Terahertz Polaritonic Meta-Atoms

Volume 12, Number 5, October 2020

Moritz Wenclawiak  
 Aaron M. Andrews  
 Gottfried Strasser  
 Karl Unterrainer  
 Juraj Darmo



DOI: 10.1109/JPHOT.2020.3021464

# Superradiant Ensembles of Terahertz Polaritonic Meta-Atoms

**Moritz Wenclawiak<sup>ID</sup>,<sup>1</sup> Aaron M. Andrews,<sup>2</sup> Gottfried Strasser,<sup>2</sup> Karl Unterrainer,<sup>1,2</sup> and Juraj Darmo<sup>1</sup>**

<sup>1</sup>Photonics Institute - TU Wien, 1040 Vienna, Austria

<sup>2</sup>Institute of Solid State Electronics, and Center for Micro-, and Nanostructures - TU Wien, 1040 Vienna, Austria

DOI:10.1109/JPHOT.2020.3021464

This work is licensed under a Creative Commons Attribution 4.0 License. For more information, see <https://creativecommons.org/licenses/by/4.0/>

Manuscript received August 12, 2020; accepted August 26, 2020. Date of publication September 3, 2020; date of current version October 2, 2020. This work was partial supported by Austrian Science Fund (FWF) through DK CoQus (W1210) and ERA.NET RUS PLUS through project COMTERA (FFG 849614). Corresponding author: Moritz Wenclawiak (e-mail: moritz.wenclawiak@tuwien.ac.at).

**Abstract:** We experimentally demonstrate the robustness of strong light-matter interaction in an ensemble of terahertz cavities with variable radiation loss. Each cavity in the form of a planar metallic resonator is strongly coupled to intersubband transitions of semiconductor quantum wells. The polariton spectra, measured by time-domain spectroscopy, do not diminish when the cavity ensemble is brought to the superradiant regime with a radiative loss rate increased by a factor of three. In contrast, the splitting of the polariton frequencies gets larger, and indicates an increased vacuum Rabi frequency. We attribute the observed phenomenon to this well-known many-body effect in quantum electrodynamics, but here associated to an ensemble of otherwise independent polariton systems.

**Index Terms:** Metamaterials, strong light-matter interaction, superradiance, terahertz, Time-domain-Spectroscopy.

## 1. Introduction

Interaction mechanisms of light and matter have sparked the curiosity of researchers over centuries. The development of cavity quantum electrodynamics (cQED) lead to prospering research in theory and experiment of what nowadays mostly is considered as coupling. Within cQED photons coupled to polar transitions are shifted to a quantum regime, which is usually described on the basis of polaritons - bosonic quasiparticles which are partly light and partly matter. In recent years, the border was crossed from a solely theoretical description towards real devices harvesting this bosonic nature of polaritons [1]. It was followed by the development of polariton lasers [2] and light emitting diodes [3], [4]. Additionally, recent results show the manipulation of material properties and modified transport phenomena [5]–[7].

The coupling of light and matter is described by a parameter called coupling strength  $g$ . As a figure of merit, this is usually normalized to the bare transition  $\omega_{12}$  (or modal energy  $\omega_{\text{cav}}$ ) of the investigated system. This ratio defines the coupling regime the experiment is situated in (i.e. weak, strong or even ultrastrong coupling) and it can approach values close to unity (see e.g. reviews [8]–[10]), which is followed by the prediction of completely new physical phenomena [11]–[13].

In recent years, two particular systems emerged providing access to the ultrastrong coupling regime: On the one hand, the development of superconducting circuits lead to the possibility of

reaching coupling ratios close to unity [14], [15]. On the other hand, quantum-wells (QWs) in semiconductor heterostructures feature all the fundamental requirements to enable strong coupling experiments in a solid state environment. The huge dipole moments in intersubband transitions (ISBTs) [16], together with the increased number of contributing electrons, has lead to observations of intersubband polaritons in these kind of systems [17], [18]. In combination with an external magnetic field, the study of cyclotron resonances found record high coupling strengths [19], [20], as well as superradiant features [21], [22]. In order to observe intersubband polaritons, the interplay between coupling strength, transition (cavity) frequency and their corresponding energy loss rates is crucial.

The system investigated here features two different entities of multiple elements: Firstly, the electron ensemble, which is well known in the strong coupling regime [12], [23]–[25]. Secondly, the array of (in this case metamaterial) cavities, which is usually treated to be without self-interaction. Nevertheless, it has been shown, that this assumption is not always valid depending on the chosen arrangement [26]–[28].

The question arises what happens if both contributions, stemming from the multiple electrons and the interacting cavities, are significant. If the system's response is not only a feature of the interacting electron ensemble but is supported by a cooperative cavity behaviour, it will be possible to gain control over the strongly coupled system by controlling the array of interacting cavities itself. In this way, we are able to access quantum experiments with a tunable interaction strength but without the necessity of addressing the electron ensemble. In contrast, the cavity ensemble is easily modified by means of standard fabrication techniques which might lead to important consequences for possible future devices. The investigation of a multiple cavity experiment in the strong coupling regime is the focus of this work and will be explained in the following.

## 2. Theory & Methods

The theory of light matter coupling is usually based on finding the eigenenergies of a Hamiltonian described by a  $2 \times 2$  matrix (strong coupling, see e.g. [29]) or when reaching the ultrastrong coupling by a  $4 \times 4$  matrix Hamiltonian [11] obtained via Bogoliubov transformation [30]. Allowing the system to dissipate energy is in general included by introducing imaginary loss rates [31]  $\gamma_{\text{cav}}$  &  $\gamma_{12}$ , which, as a phenomenological approach, results in a non-Hermitian Hamiltonian. However, it can be modelled based on quantum Langevin equations, introducing coupling terms corresponding to photonic and electronic reservoirs [12]. Nevertheless, signatures of the ultrastrong coupling regime, i.e. the inclusion of an asymmetric polariton dispersion due to terms stemming from the squared vector potential, are expected to be observable when reaching coupling ratios above 0.5 [11], which is a number exceeding the results presented in this work. Therefore, we choose a theoretical foundation based on cQED and a general  $2 \times 2$  matrix approach as described in [29].

In this description, the introduced loss rates lead to the constraint

$$\frac{\gamma_{\text{cav}} + \gamma_{12}}{4} < g = \hbar\Omega_R \quad (1)$$

for the coupling parameter, which is usually expressed in terms of the vacuum Rabi frequency  $\Omega_R$ , in order to observe the splitting into two intersubband polariton branches. If (1) is violated, the system is shifted to the weak coupling regime. In this contribution, we want to focus on modified cavity losses  $\gamma_{\text{cav}}$  due to the increased radiation loss when arranging them in subwavelength ensembles [26]. This behaviour is analogous to superradiantly emitting atoms in a confined volume [23], [32]. Therefore, the influence of the cavity linewidth on the coupled system, i.e. on the polariton formation, is investigated.

Cavities used in the THz regime for strong coupling experiments are usually made of single- or double-metal (gold) waveguides. In this case, we use planar gold structures as the basic building block of a metamaterial surface [33], [34]. Many strong coupling experiments in the THz frequency range are performed with split ring resonators [35], [36] or their complementary counter parts [37].

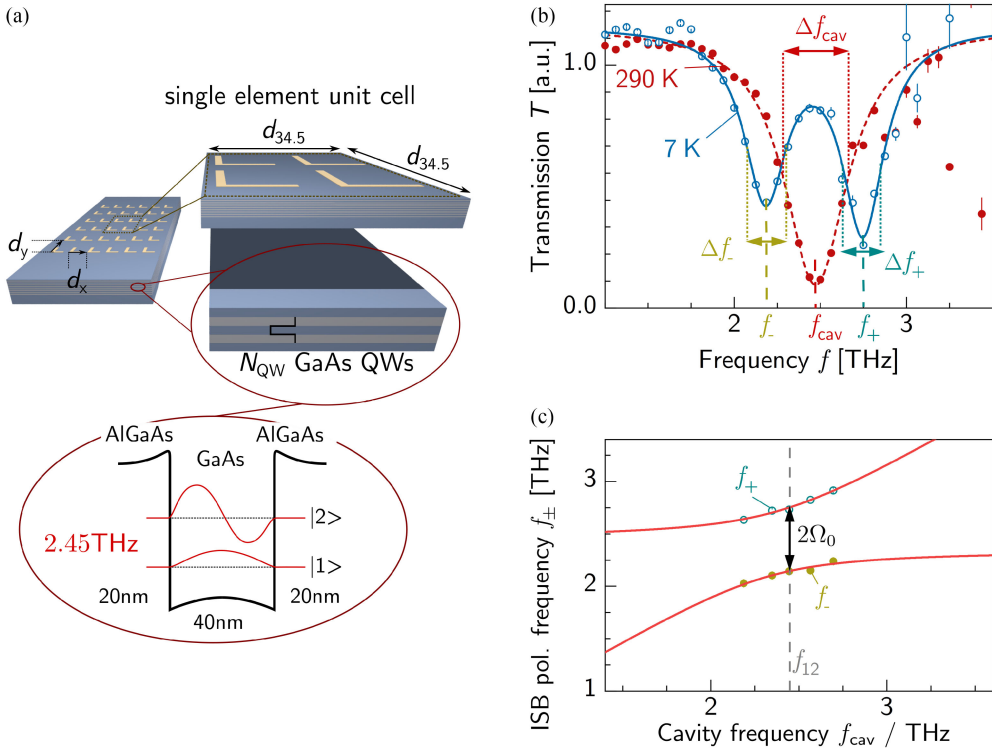


Fig. 1. Characterisation of the investigated system. a) Sample layout:  $N$  (in this case  $N = 4$ ) elements are arranged in unit cells whose area determine the number of subwavelengthly confined elements. The  $2 \rightarrow 1$  ISBT in the QW (expected at  $f_{12} = 2.45$  THz) couples to the z-component of the electric field of the deposited planar metallic resonator. b) The obtained transmission spectra showing the resonator response (290 K) and the strong coupling regime (7 K). The viewgraph shows all the extracted parameters for a (sum of) Lorentzian fit(s). c) Mapping the polariton dispersion by varying the resonator dimension shows the expected anticrossing behaviour and verifies  $f_{12} = 2.42$  THz.

Reflection experiments mostly feature double-metal patch resonators [38], [39] or specially engineered LC cavities [40]–[42]. The cavity losses usually do not enter any consideration as long as (1) is fulfilled, otherwise the system is expected to merge to the weakly coupled case.

Although there are experiments approaching the few electron limit [43], [44], the typical number of interacting electrons exceeds one by orders of magnitude  $n_{\text{el}} \gg 1$ . For  $n_{\text{el}}$  electrons interacting with a single mode radiation field  $\Omega_R \propto \sqrt{n_{\text{el}}}$  [24]. In the experimental part, we only use one type of resonator, which is why we will define the expression

$$\Omega_0 \propto \sqrt{\frac{n_{\text{el}}}{V}} = \text{const.} \quad (2)$$

as the single resonator vacuum Rabi frequency featuring a constant number of interacting electrons in a given (cavity electric field dependent) mode volume  $V$ . (The definition of  $V$  is a topic heavily discussed even in recent research [45]–[48].) In general, we are only able to discriminate modifications of the ratio  $n_{\text{el}}V^{-1}$ .

Our samples consist of arrays of planar gold resonators, as depicted in figure 1(a), fabricated via conventional photolithography and deposited on a heterostructure featuring  $N_{\text{QW}} = 30$  Gallium-Arsenide QWs with a width of 40 nm separated by 20 nm wide Aluminium-Gallium-Arsenide barriers with an Aluminium content of 15% and a  $2 \rightarrow 1$  frequency expected to be positioned at  $f_{12} \approx 2.45$  THz. The array parameter  $d_{x,y}$  is varied in order to modify the radiative losses of the system, but the resonator dimensions are kept constant, as far as possible, featuring a first order

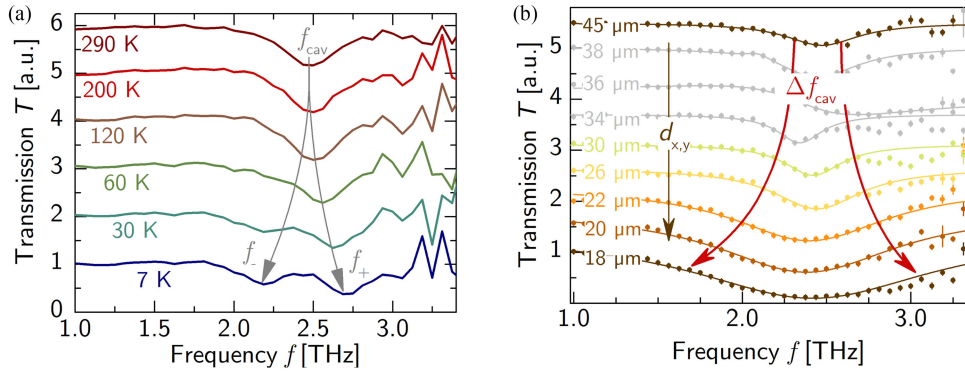


Fig. 2. Temperature response of the investigated samples. a) At room temperature, the coupling is switched off due to sufficient electron energies, which enables the characterisation of the cavity. Below  $T_K < 120$  K the ISB polaritons start to be observable. b) Transmission spectra of the resonator response for the decreasing array parameter  $d_{x,y}$  measured at 290 K. Cavity losses  $\Delta f_{\text{cav}}$  are increasing for increasing number of elements in the unit cell from top to bottom. (Spectra distorted by the interaction with the lattice mode [55] are shown in gray.)

resonance at  $f_{\text{cav}} \approx 2.45$  THz. (We hereby have to slightly modify the length in order to compensate for the blueshift introduced by the change of  $d_{x,y}$  [49].)

All spectra are recorded via time-domain spectroscopy (TDS) [50] with the sample placed in a liquid helium (LHe) flow cryostat. Broadband THz radiation is emitted by a large area photoconductive antenna [51], [52] and detected after transmission through the sample via electro-optic sampling [53], [54]. For LHe temperatures, we expect all electrons to be in the ground state  $|1\rangle$  of the quantum well, hence we can observe strong coupling between the plasmonic resonator and the ISBT in the transmission spectra (derived from a comparison to an unprocessed QW sample); the room temperature spectra yield information of the bare cavity properties (figure 1(b)). We include in the viewgraph (b) all the parameters we retrieve out of fitting a (sum of) Lorentzian distribution function(s), i.e. frequency position of the cavity  $f_{\text{cav}}$  and polaritons  $f_{\pm}$  (−: lower polariton, +: upper polariton) and their linewidths  $\Delta f_{\text{cav},\pm}$ , respectively. As  $\sum \Delta f_{\pm} = \Delta f_{\text{cav}}$ , we can neglect the loss mechanisms in the heterostructure, so (1) is solely determined by the cavity losses  $\gamma_{\text{cav}}$ . We estimate a value of  $\Omega_0 = 0.29 \pm 0.03$  THz for the intrinsic vacuum Rabi frequency.

The polariton dispersion is mapped by modifying the cavity length and hence the resonance frequency (figure 1(c)). It features the expected anti-crossing response when sweeping through the ISBT frequency, which is determined to be positioned at  $f_{12} = 2.42$  THz as expected. So far, we are clearly in the regime in which (1) is fulfilled. We will now modify the cavity losses by increasing the number of resonators in the ensemble.

### 3. Results

In order to characterize the cavity, we map the temperature response from 290 K down to 7 K as shown in figure 2(a). 2.5 THz correspond to an equivalent temperature of  $T_{K,2.5} \approx 120$  K, which is why we do not expect a modification for  $T_K > 120$  K. When approaching LHe temperature the formation of the two ISB polariton branches is observable. Hence, the room temperature measurements enable a complete characterization of the cavity response, which is presented in the following.

For large resonator separations, the system is expected to show the intrinsic response of a single cavity. We define the single element unit cell as  $d_{34.5} \times d_{34.5}$ , which hereby is depending on  $f_{\text{cav}}$  and the refractive index of the substrate  $n = 3.6$  at 2.5 THz [56] via  $c(f_{\text{cav}}n)^{-1} = \lambda_{\text{cav}} = d_{34.5}$ . Increasing the number of cavities in these cells is then expected to show an enhanced radiation loss manifesting in an increased linewidth of the resonance features in the transmission spectra [26].

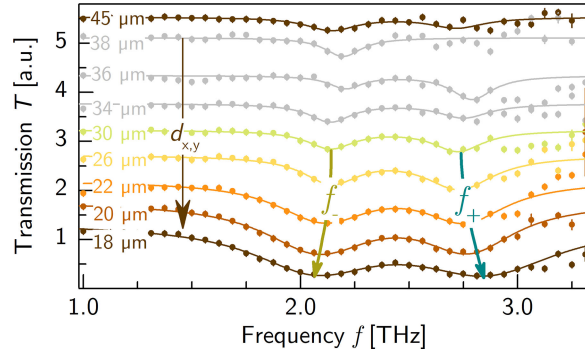


Fig. 3. Transmission spectra measured at  $T_K = 7$  K. Although the cavity loss are increased by a factor of 3, it is still possible to observe the ISB polaritons as a signature of the strong coupling regime.

This is shown in figure 2(b). When decreasing  $d_{x,y}$ , it is possible to observe an increase of  $\Delta f_{\text{cav}}$ . We have to stress, that this cooperative response is solely caused by the subwavelength arrangement and not affected by the QWs, as the two systems are decoupled at room temperature.

In addition, the transmission dip shows distortions from the, otherwise Lorentzian, response for values in proximity to the so called lattice mode [55], which is why we mark them gray.

We determine the intrinsic response for samples with a resonator number  $N \leq 1$  per unit-cell. As a result, we measure an intrinsic linewidth of  $\Delta f_0 = 480 \pm 50$  GHz. For  $N > 1$ , the cavities follow the linear approximation  $\Delta f_{\text{cav}} = N\Delta f_0$  [57] which is in good agreement to our study performed in a scenario without strong light-matter interaction [26].

In order to investigate the effects of the superradiant cavity response on the strongly coupled system, we measure the transmission spectra at 7 K, which is plotted in Fig 3. Two important features are observable: Firstly, the polariton linewidths broaden symmetrically for a decreasing  $d_{x,y}$ . It justifies our prior assumption, that the coupling term in the Hamiltonian is symmetric and that the contributions of the USC regime are negligible. Secondly, the polaritons are robust against any modification of the metamaterial array. This is a surprising result, especially for the samples showing a significant linewidth broadening. Since the linewidth of the bare cavity resonance  $\Delta f_{\text{cav}}$  is increasing for the confined cavities by a maximum factor of 3, one would expect a transition towards the weak coupling regime because (1) is violated. In contrast, the transmission spectra even show an increased splitting between upper and lower polariton frequency.

#### 4. Discussion

We use the spectra to obtain the polariton parameters as written in 2. First, we compare the polariton frequencies in figure 4(a). As mentioned before, they are expected to show a symmetric response, which is indeed the case. Increasing the cavity loss leads to a violation of (1), marked as vertical dashed black line. This is the limit of the strong coupling regime, i.e. on its right hand side the vacuum Rabi frequency does not exceed the overall losses of the system, which according to theory makes it impossible to observe ISB polaritons. Nevertheless, we maintain the strong coupling between metamaterial surface and ISBT, which has severe consequences for  $\Omega_R$  itself.

Due to (2), the interaction strength between a single cavity and the ISBT is fixed. Contrary to that, our previous discussion showed that even for losses exceeding the intrinsic value of  $\Omega_0$  the observation of ISB polaritons is still possible. Therefore, only an increased value of  $\Omega_R$  is able to maintain the polariton formation. We attribute this to the multiple cavity metamaterial surface featuring a superradiant response. As the radiative loss is modified by the entity of elements scaling with  $\sqrt{N}$ , the usual assumption of independent cavities has to be dropped.

The parameters extracted at room- and LHe temperature enable the determination of  $\Omega_R$  for each sample. These are shown in figure 4(b). They are calculated independently for both ISB polaritons

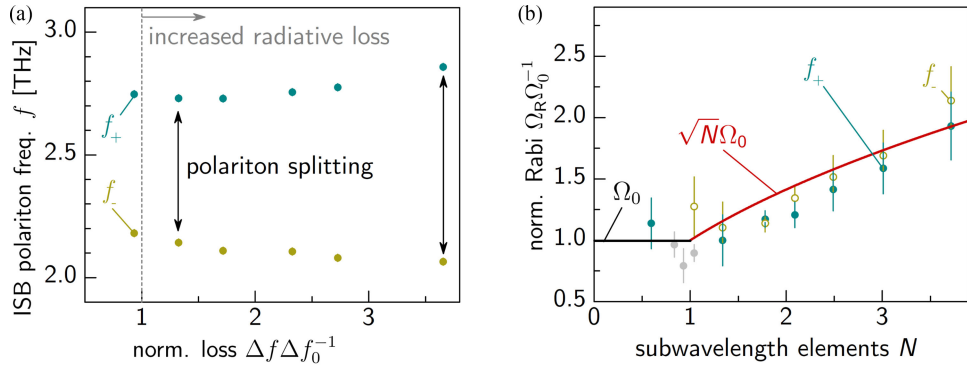


Fig. 4. a) The ISB polariton frequencies extracted of the transmission spectra against the normalized loss of the planar resonators. When the radiative loss exceeds the intrinsic loss  $\Delta f_0$  the ISB polaritons are expected to diminish. In contrast, the ISB polariton splitting even increases. b) The extracted parameters enable the calculation of the vacuum Rabi frequency  $\Omega_R$ . For  $N < 1$  element(s) per unit cell, the system shows the intrinsic vacuum Rabi frequency  $\Omega_0$ . For increasing  $N$  the values follow a dependency of  $\sqrt{N} \Omega_0$  (solid red line), which is in agreement with the superradiant radiation loss rate of the multiple cavity metasurface.

taking into account their individual frequency and linewidth. We hereby normalize the values to  $\Omega_0$  and plot them for against the number of elements in the unit cell. It is visible that for  $N > 1$ , the extracted values of  $\Omega_R$  increase with the number of interacting cavities. The vacuum Rabi frequency hereby follows the same  $\sqrt{N}$  behaviour as the superradiant metamaterial surface (included as solid red lines). This scaling bears the analogy to multi-particle treatments in cQED [24], whereas the ensemble is represented by multiple polaritonic meta-atoms, i.e. an entity of strongly coupled systems. A comparable density dependent response of the vacuum Rabi frequency has been observed in a slightly different experiment using split ring resonator ensembles on a metamaterial surface placed in a THz photonic cavity [28]. Therefore, we state that for a surface consisting of subwavelengthly arranged polaritonic meta-atoms, the independent cavity assumption, as the state of the art approach for describing strongly coupled systems in the THz regime, is not valid.

An important consequence of our observation is that for a planar metamaterial surface consisting of several elements, it might be even more favourable to use a dense array in order to benefit from an improved amplitude response. Despite the modified radiation loss, the polariton splitting is still observable. In fact, it is increased because of the enhanced light-matter interaction due to the modified response within the ensemble of polaritonic meta-atoms.

We can estimate the maximum vacuum Rabi frequency  $\Omega_{\max} \approx 0.56$  THz, yielding  $\Omega_{\max} f_{12}^{-1} \approx 23\%$ , which is significantly higher than the single resonator response  $\Omega_0 f_{12}^{-1} \approx 12\%$ . Therefore, increased interaction strengths are feasible with a superradiant ensemble of elements. However, when approaching the USC regime, a full analysis requires a mapping of the polariton dispersion in dependence of the detuning between ISBT- and resonator frequency similar to the one presented in 2 to take into account possible contributions of the squared vector potential in the Hamiltonian [11], [12].

## 5. Conclusion

In conclusion, we use a metamaterial surface consisting of THz cavities arranged in a subwavelength geometry in order to modify their radiative response. By coupling the cavities to a frequency matched ISBT in a semiconductor heterostructure, a system which we call polaritonic meta-atom, we are able to reach a coupling ratio between vacuum Rabi- and transition frequency of 12% in the limit of a single polaritonic meta-atom or non-interacting cavities, respectively. Increasing the density of polaritonic meta-atoms is directly followed by an increased radiation loss due to the

subwavelength confinement. Nevertheless, the strong coupling between the metasurface and ISBT remains robust although the overall losses of the system are increased by a factor of 3. The reason is the interaction within the ensemble of resonators, which forces to drop the assumption of multiple independent cavities each interacting with a huge number of electrons as the common description for these type of systems. Therefore, the general treatment has to be expanded to a multiple cavity - multiple electron interaction picture. The experimental results show that it is possible to influence the strongly coupled system by manipulating the array of cavities itself. Therefore, the problem of gaining control over devices operating in the strong coupling regime can be shifted to a scale more feasible in modern fabrication technology. Additionally, it enables the observation of increased interaction strengths, in this case the maximum coupling ratio is determined to be 23%, without compromising the amplitude of the detected signal.

## References

- [1] A. Imamoğlu, R. Ram, S. Pau, and Y. Yamamoto, "Nonequilibrium condensates and lasers without inversion: Exciton-polariton lasers," *Phys. Rev. A*, vol. 53, no. 6, p. 4250, 1996.
- [2] C. Schneider *et al.*, "An electrically pumped polariton laser," *Nature*, vol. 497, no. 7449, pp. 348–352, May 2013.
- [3] D. Bajoni, "Polariton lasers. Hybrid light-matter lasers without inversion," *J. Physics D: Appl. Physics*, vol. 45, no. 40, p. 409501, Oct. 2012.
- [4] S. Tsintzos, N. Pelekanos, G. Konstantinidis, Z. Hatzopoulos, and P. Savvidis, "A gaas polariton light-emitting diode operating near room temperature," *Nature*, vol. 453, no. 7193, pp. 372–375, 2008.
- [5] E. Orgiu *et al.*, "Conductivity in organic semiconductors hybridized with the vacuum field," *Nature Materials*, vol. 14, no. 11, pp. 1123–1129, 2015.
- [6] D. Hagenmüller, J. Schachenmayer, S. Schütz, C. Genes, and G. Pupillo, "Cavity-enhanced transport of charge," *Phys. Rev. Lett.*, vol. 119, p. 223601, Nov 2017.
- [7] G. L. Paravicini-Bagliani *et al.*, "Magneto-transport controlled by landau polariton states," *Nature Phys.*, vol. 15, no. 2, pp. 186–190, 2019.
- [8] D. G. Baranov, M. Wersäll, J. Cuadra, T. J. Antosiewicz, and T. Shegai, "Novel nanostructures and materials for strong light-matter interactions," *ACS Photon.*, vol. 5, no. 1, pp. 24–42, 2018.
- [9] P. Forn-Díaz, L. Lamata, E. Rico, J. Kono, and E. Solano, "Ultrastrong coupling regimes of light-matter interaction," *Rev. Modern Phys.*, vol. 91, no. 2, p. 025005, 2019.
- [10] A. F. Kockum, A. Miranowicz, S. De Liberato, S. Savasta, and F. Nori, "Ultrastrong coupling between light and matter," *Nature Rev. Phys.*, vol. 1, no. 1, pp. 19–40, 2019.
- [11] C. Ciuti, G. Bastard, and I. Carusotto, "Quantum vacuum properties of the intersubband cavity polariton field," *Phys. Rev. B*, vol. 72, no. 11, p. 115303, 2005.
- [12] C. Ciuti and I. Carusotto, "Input-output theory of cavities in the ultrastrong coupling regime: The case of time-independent cavity parameters," *Phys. Rev. A*, vol. 74, no. 3, p. 033811, 2006.
- [13] R. Stassi, A. Ridolfo, O. Di Stefano, M. J. Hartmann, and S. Savasta, "Spontaneous conversion from virtual to real photons in the ultrastrong-coupling regime," *Phys. Rev. Lett.*, vol. 110, no. 24, p. 243601, 2013.
- [14] P. Forn-Díaz *et al.*, "Observation of the Bloch-Siegert shift in a qubit-oscillator system in the ultrastrong coupling regime," *Phys. Rev. Lett.*, vol. 105, no. 23, p. 237001, 2010.
- [15] T. Niemczyk *et al.*, "Circuit quantum electrodynamics in the ultrastrong-coupling regime," *Nature Phys.*, vol. 6, no. 10, pp. 772–776, 2010.
- [16] M. Helm, "Intersubband Transitions in Quantum Wells," in *Physics and Device Appl.*, ser. Semiconductors and Semimetals. San Diego: Academic Press, 2000, vol. 62.
- [17] A. Liu, "Rabi splitting of the optical intersubband absorption line of multiple quantum wells inside a Fabry-Pérot microcavity," *Phys. Rev. B*, vol. 55, no. 11, p. 7101, 1997.
- [18] D. Dini, R. Köhler, A. Tredicucci, G. Biasiol, and L. Sorba, "Microcavity polariton splitting of intersubband transitions," *Phys. Rev. Lett.*, vol. 90, no. 11, p. 116401, 2003.
- [19] G. Scalari *et al.*, "Ultrastrong coupling of the cyclotron transition of a 2d Electron Gas to a THz Metamaterial," *Sci.*, vol. 335, no. 6074, pp. 1323–1326, 2012.
- [20] A. Bayer, M. Pozimski, S. Schambeck, D. Schuh, R. Huber, D. Bougeard, and C. Lange, "Terahertz light-matter interaction beyond unity coupling strength," *Nano Lett.*, vol. 17, no. 10, pp. 6340–6344, 2017.
- [21] Q. Zhang *et al.*, "Superradiant decay of cyclotron resonance of two-dimensional electron gases," *Phys. Rev. Lett.*, vol. 113, no. 4, p. 047601, 2014.
- [22] Q. Zhang *et al.*, "Collective non-perturbative coupling of 2d electrons with high-quality-factor terahertz cavity photons," *Nature Phys.*, vol. 12, no. 11, pp. 1005–1011, 2016.
- [23] R. H. Dicke, "Coherence in spontaneous radiation processes," *Phys. Rev.*, vol. 93, no. 1, pp. 99–110, 1954.
- [24] M. Tavis and F. W. Cummings, "The exact solution of N two level systems interacting with a single mode, quantized radiation field," *Physics Lett. A*, vol. 25, no. 10, pp. 714–715, 1967.
- [25] A. Vasanelli, Y. Todorov, and C. Sirtori, "Ultra-strong light-matter coupling and superradiance using dense electron gases," *Comptes Rendus Physique*, vol. 17, no. 8, pp. 861–873, 2016.
- [26] M. Wenclawiak, K. Unterrainer, and J. Darmo, "Cooperative effects in an ensemble of planar meta-atoms," *Appl. Physics Lett.*, vol. 110, no. 26, p. 261101, 2017.

- [27] J. Keller *et al.*, "Superradiantly limited linewidth in complementary THz metamaterials on si-membranes," *Adv. Opt. Mater.*, vol. 6, no. 16, p. 1800210, 2018.
- [28] F. Meng, M. D. Thomson, B. Klug, D. Čibiraitė, Q. Ul-Islam, and H. G. Roskos, "Nonlocal collective ultrastrong interaction of plasmonic metamaterials and photons in a terahertz photonic crystal cavity," *Opt. Express*, vol. 27, no. 17, pp. 24 455–24 468, 2019.
- [29] L. C. Andreani, G. Panzarini, and J.-M. Gérard, "Strong-coupling regime for quantum boxes in pillar microcavities: Theory," *Phys. Rev. B*, vol. 60, no. 19, p. 13276, 1999.
- [30] N. N. Bogoljubov, "A new method in the theory of superconductivity," *Fortschritte der physik*, vol. 6, no. 11–12, pp. 605–682, 1958.
- [31] C. Cohen-Tannoudji, B. Diu, and F. Laloë, *Quantum Mechanics Vol. 1*. New York: Wiley, 2003.
- [32] N. Skribanowitz, I. P. Herman, J. C. MacGillivray, and M. S. Feld, "Observation of Dicke superradiance in optically pumped HF gas," *Phys. Rev. Lett.*, vol. 30, no. 8, pp. 309–312, 1973.
- [33] V. G. Veselago, "The electrodynamics of substances with simultaneously negative values of epsilon and mu," *Soviet Phys. Uspekhi*, vol. 10, no. 4, pp. 509–514, 1968.
- [34] J. B. Pendry, A. J. Holden, W. J. Stewart, and I. Youngs, "Extremely low frequency plasmons in metallic mesostructures," *Phys. Rev. Lett.*, vol. 76, no. 25, pp. 4773–4776, Jun. 1996.
- [35] D. Dietze, A. Benz, G. Strasser, K. Unterrainer, and J. Darmo, "Terahertz meta-atoms coupled to a quantum well intersubband transition," *Opt. Express*, vol. 19, no. 14, pp. 13 700–13 706, 2011.
- [36] D. Dietze, A. M. Andrews, P. Klang, G. Strasser, K. Unterrainer, and J. Darmo, "Ultrastrong coupling of intersubband plasmons and terahertz metamaterials," *Appl. Phys. Lett.*, vol. 103, no. 20, p. 201106, 2013.
- [37] C. Maissen *et al.*, "Ultrastrong coupling in the near field of complementary split-ring resonators," *Phys. Rev. B*, vol. 90, no. 20, p. 205309, 2014.
- [38] Y. Todorov *et al.*, "Ultrastrong light-matter coupling regime with polariton dots," *Phys. Rev. Lett.*, vol. 105, no. 19, p. 196402, 2010.
- [39] B. Askenazi *et al.*, "Ultra-strong light–matter coupling for designer Reststrahlen band," *New J. Phy.*, vol. 16, no. 4, p. 043029, 2014.
- [40] M. Geiser, F. Castellano, G. Scalari, M. Beck, L. Nevou, and J. Faist, "Ultrastrong coupling regime and plasmon polaritons in parabolic semiconductor quantum wells," *Phys. Rev. Lett.*, vol. 108, no. 10, p. 106402, 2012.
- [41] A. Benz, S. Campione, J. F. Klem, M. B. Sinclair, and I. Brener, "Control of strong light–matter coupling using the capacitance of metamaterial nanocavities," *Nano Lett.*, vol. 15, no. 3, pp. 1959–1966, 2015.
- [42] M. Jeannin *et al.*, "Ultrastrong light–matter coupling in deeply subwavelength THz LC resonators," *ACS Photon.*, vol. 6, no. 5, pp. 1207–1215, 2019.
- [43] Y. Todorov and C. Sirtori, "Few-electron ultrastrong light-matter coupling in a quantum LC Circuit," *Phys. Rev. X*, vol. 4, no. 4, 2014.
- [44] J. Keller *et al.*, "Few-electron ultrastrong light-matter coupling at 300 GHz with nanogap hybrid LC microcavities," *Nano Lett.*, vol. 17, no. 12, pp. 7410–7415, 2017.
- [45] E. M. Purcell, H. C. Torrey, and R. V. Pound, "Resonance absorption by nuclear magnetic moments in a solid," *Phys. Rev.*, vol. 69, no. 1–2, p. 37, 1946.
- [46] K. J. Vahala, "Optical Microcavities," *Nature*, vol. 424, no. 6950, pp. 839–846, 2003.
- [47] P. T. Kristensen, C. Van Vlack, and S. Hughes, "Generalized effective mode volume for leaky optical cavities," *Opt. Lett.*, vol. 37, no. 10, p. 1649, 2012.
- [48] P. T. Kristensen and S. Hughes, "Modes and mode volumes of leaky optical cavities and plasmonic nanoresonators," *ACS Photon.*, vol. 1, no. 1, pp. 2–10, 2014.
- [49] R. Singh, C. Rockstuhl, and W. Zhang, "Strong influence of packing density in terahertz metamaterials," *Appl. Phys. Lett.*, vol. 97, no. 24, p. 241108, 2010.
- [50] D. Grischkowsky, S. Keiding, M. v. Exter, and C. Fattinger, "Far-infrared time-domain spectroscopy with terahertz beams of dielectrics and semiconductors," *JOSA B*, vol. 7, no. 10, pp. 2006–2015, 1990.
- [51] D. H. Auston, K. P. Cheung, and P. R. Smith, "Picosecond photoconducting Hertzian dipoles," *Appl. Phys. Lett.*, vol. 45, no. 3, p. 284, 1984.
- [52] A. Dreyhaupt, S. Winnerl, T. Dekorsy, and M. Helm, "High-intensity terahertz radiation from a microstructured large-area photoconductor," *Appl. Phys. Lett.*, vol. 86, no. 12, p. 121114, 2005.
- [53] Q. Wu and X.-C. Zhang, "Design and characterization of traveling-wave electrooptic terahertz sensors," *IEEE J. Sel. Topics Quantum Electron.*, vol. 2, no. 3, pp. 693–700, Sep. 1996.
- [54] A. Leitenstorfer, S. Hunsche, J. Shah, M. C. Nuss, and W. H. Knox, "Detectors and sources for ultrabroadband electro-optic sampling: Experiment and theory," *Appl. Phys. Lett.*, vol. 74, no. 11, pp. 1516–1518, 1999.
- [55] A. Bitzer, J. Wallauer, H. Helm, H. Merbold, T. Feurer, and M. Walther, "Lattice modes mediate radiative coupling in metamaterial arrays," *Opt. Express*, vol. 35, no. 23, pp. 3859–3861, 2009.
- [56] E. D. Palik and G. Ghosh, Eds., *Handbook Optical Constants Solids*. San Diego: Academic Press, 1998.
- [57] A. V. Andreev, V. I. Emel'yanov, and Y. A. Il'inskii, *Cooperative effects optics*, ser. Malvern physics series. Bristol and Philadelphia: IOP Publishing, 1993.